A4: Hall Effect
Semiconductor Physics I - Laboratory

Hassan Tanveer - 3735258, Simon Briesenick - 3712933
Experiment conducted on: 23.November 2020

I. Abstract

Several probes were investigated. The ionization energy of an unknown donor was estimated in a ZnO bulk and a PLD grown thin film sample. For the thin film, corrections for the mobility and carrier concentration were needed. The mobility was found to agree with theoretical predictions for ZnO, in particular the three most dominant scattering mechanisms (ionized impurity, piezoelectric and deformation potential scattering) in bulk ZnO could be matched to high accuracy, while for the thin film sample, two similar scattering mechanisms were fit for the mobility at low temperatures. The donor ionization energy for the bulk sample was determined to be $E_D^b = 35 \pm 0.5eV$, while for the thin film, we found $E_D^b = 37 \pm 1eV$. These results agree very well with those of others, most notably with [10] and [13], where the donor was proposed to be interstitial Hydrogen. These ionization energies are also in relative proximity to the ionization energy for the simple hydrogenic model for shallow donor states in ZnO $E_D^b \cong 42meV$. The donor concentration N_D was obtained for bulk and thin film ZnO to be $N_D = (1.17 \pm 0.05) \times 10^{17} cm^{-3}$ and $N_D = (1.70 \pm 0.05) \times 10^{18} cm^{-3}$, respectively. Before presenting the results, we discussed the important theoretical framework, such as carrier statistics and scattering mechanisms, as well as the experimental setup we used to obtain these results.

II. Introduction

A. Theoretical Background

1) Classical Treatment of charges in $\vec{E}$ and $\vec{B}$ fields: In free space, the movement of a charge q, subject to $\vec{E} = E\vec{e_x}$ and $\vec{B} = B\vec{e_z}$ fields is determined by the Lorentz Force:

$$\vec{F} = m\dot{\vec{v}} = q(\vec{E} + \vec{v} \times \vec{B}) \tag{1}$$

The solution for the EOM is the so-called cyclotron motion, which is a superposition of a circular motion in the plane of the magnetic field with angular frequency $\omega_c = qB/m$ and a linear motion perpendicular to both fields with velocity $v = E/B$. This superposition leads to cyclotron motion along the equipotential lines of the fields.

In a crystal, the situation is different. Firstly, the mass of the charge carrier needs to be replaced by the effective mass m_e. The effective mass incorporates the effects of the rigid periodic potential and is valid for charge carriers sufficiently close to the band gap (invocation of parabolic edge approximation). Secondly, the crystal is never perfect and scattering of charge carriers with phonons, lattice defects, other electrons or impurity atoms can further decrease the ability of constant acceleration. This effect is captured by the impulse relaxation time τ - a measure for the time between collisions. Hence, the Lorentz Force is modified to read:

$$\begin{aligned} \vec{F} &= \left(\frac{d\vec{p}}{dt}\right)_{Scattering} + \left(\frac{d\vec{p}}{dt}\right)_{Fields} \\ &= \frac{m_e\vec{v}}{\tau} + q(\vec{E} + \vec{v} \times \vec{B}) \end{aligned} \tag{2}$$

In equilibrium, $\vec{F} = 0$ and the solution is given by the matrix product

$$\begin{bmatrix} E_x \\ E_y \end{bmatrix} = \begin{bmatrix} m_e q/\tau & -B \\ B & m_e q/\tau \end{bmatrix} \begin{bmatrix} v_x \\ v_y \end{bmatrix} \tag{3}$$

It can alternatively also be written in the form of Ohm's law $\vec{E} = \rho\vec{j}$ with $\vec{j}$ being the current density, resulting from the product of charge density n, q and the drift velocity $\vec{j} = nq\langle\vec{v}\rangle$:

$$\begin{bmatrix} E_x \\ E_y \end{bmatrix} = \sigma_0^{-1} \begin{bmatrix} 1 & -\omega_c\tau \\ \omega_c\tau & 1 \end{bmatrix} \begin{bmatrix} j_x \\ j_y \end{bmatrix} \tag{4}$$

with conductivity $\sigma_0 = q^2 n\tau/m_e$. The off-diagonal terms in eqns. (3) and (4) indicate the extent by which the magnetic field can cause the charges to move perpendicular to the applied electric field.

In a semiconducting bar fixed in an electromagnetic field with electric and magnetic fields at right angles to each other as described above (i.e. with $\vec{E} = E\vec{e_x}$ and $\vec{B} = B\vec{e_z}$) (see Fig. 1), charge will build up on either side of the bar. This accumulated charge is what induces the transverse Hall field E_H. The steady state condition is reached, when the Hall field has built up to the extent that the deflection caused by the magnetic field is exactly counteracted:

$$F_y = q(E_H + (\vec{v} \times \vec{B})_y) = 0 \tag{5}$$

Alternatively, one can also demand that the carriers are only to flow in the x-direction and not in the y-direction, i.e. $j_y = 0$. Inserting this condition into eqn. (4) leads to the result:

$$E_H = \frac{U_H}{b} = \frac{j_x B}{nq} = R_H IB/d \tag{6}$$

with $R_H = 1/nq$ being the Hall coefficient. The charge density n was used here to be a placeholder for either the electron density n or the hole density p, depending on the

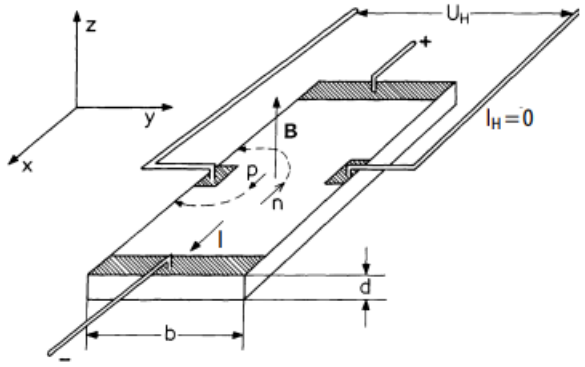

Fig. 1. Simplest, schematic setup for the classical Hall effect. Electric field $\vec{E}$ and magnetic induction $\vec{B}$ at right angles to each other. The dashed curves represent the deflections of electrons n and holes p within the probe until the transverse Hall field has build up. From [2], p. 473.

charge type, q needs to be replaced with $q = \mp e$. Note, that the discussed situation assumes only one kind of charge carrier, which is approximately true in doped semiconductors at room temperature. A more complete discussion for the case of both kinds of charge carriers can be found in [1], albeit that this is not necessary for this report.

2) Carrier concentration statistics and mobility temperature dependence: We are considering an uncompensated n-type semiconductor with a donor binding energy close to the conduction band edge, $E_D^b = E_C - E_D$. In the most simplistic model, the donor atom supports a shallow electronic state in which the electron is weakly bound in a hydrogenic configuration. In many cases, Bohr's theory of the hydrogen atom provides reasonable results, as long as the energy is scaled with the the effective mass m_e and the dielectric constant ϵ_r of the material. The ionization energy E_D^b is then given by:

$$E_D^b = \frac{m_e}{m_0}\frac{1}{\epsilon_r^2}\frac{m_0 e^4}{2(4\pi\epsilon_0\hbar)^2}. \tag{7}$$

However, the results from this model only hold for the case of *shallow* level donors and deviate significantly from *deep* level donors and semiconductors with a strongly anisotropic effective mass.

Since ZnO grows in the wurtzite crystal structure, the effective mass is uniaxially anisotropic and is equal to [7], $m_e^T = 0.24m_0$ and $m_e^L = 0.21m_0$ at or close to the Γ-point. In addition with the dielectric constant $\epsilon_r = 8.66$ [8] this serves to give a rough estimate of the ionization energy of shallow donors in ZnO to $E_D^b \cong 42meV$ (the effective mass used here was taken to be the average, i.e. $m_e = \frac{1}{3}(2m_e^T + m_e^L)$).

Electrons can be either donated to the conduction band by valence band electrons acquiring enough thermal energy to jump the gap or by weakly bound donor electrons being supplied by ionizing the donor with energy E_D^b. For the intrinsic case, the carrier concentration is given by the well known result:

$$n_i = \sqrt{N_C N_V}e^{-E_G/2k_BT} \tag{8}$$

with

$$N_C = 2\left[\frac{m_{e,n}k_BT}{2\pi\hbar^2}\right]^{3/2} \text{ and} \tag{9}$$

$$N_V = 2\left[\frac{m_{e,p}k_BT}{2\pi\hbar^2}\right]^{3/2} \tag{10}$$

being the *effective* density of conduction and valence band states. For a n-type doped semiconductor, the concentration of electrons is given by the general result:

$$n(T) = N_C(T)exp\left(\frac{E_F - E_C}{k_BT}\right) \tag{11}$$

where the Fermi level E_F will in general be a complicated function of the doping concentration of the donator atoms and the temperature. To avoid an expression of the carrier concentration in terms of the Fermi level in order to obtain a more useful empirical model, a lengthy derivation from first principles is needed. We shall quickly go over the assumptions and discuss the important implications for various temperature ranges.

For sufficiently low temperature ranges ($n_i \ll N_D, N_D$ being the donor concentration), the ratio of populations in a two-level system, is given by the Boltzmann factor, supplemented with an additional degeneracy factor $\frac{g_+}{g_0} = \hat{g}_D$:

$$\frac{N_D^0}{N_D^+} = \frac{g_+}{g_0}\exp\left(-\frac{\Delta E}{k_BT}\right) \tag{12}$$

$$= \hat{g}_D \exp\left(\frac{E_F - E_D}{k_BT}\right). \tag{13}$$

The two population densities N_D^0 and N_D^+ correspond to the number of electrically neutral and to the number of already ionized donors, respectively, such that $N_D = N_D^0 + N_D^+$. The population density of empty donors is then found to follow a logistic model:

$$N_D^+ = \frac{N_D}{1 + \hat{g}_D \exp\left(\frac{E_F - E_D}{k_BT}\right)}, \tag{14}$$

where $\hat{g}_D = 2$. By the above assumption, the electron density in the conduction band needs to be equal to the density of ionized donors. Hence, we arrive at the neutrality condition for n-type semiconductors:

$$-n + N_D^+ = 0. \tag{15}$$

This serves to eliminate the appearance of the Fermi level from eq. (11). Three (in compensated semiconductors, four) regions for the temperature are typically classified, out of which only the first one is of importance for this report. The above calculation is only reliable as long as the necessary approximations hold, which is why an equation for the carrier concentration can only be given for the first of the four regions:

- *Freeze out region (low T):*
  At $T = 0K$, all e^- occupy the lowest available energy

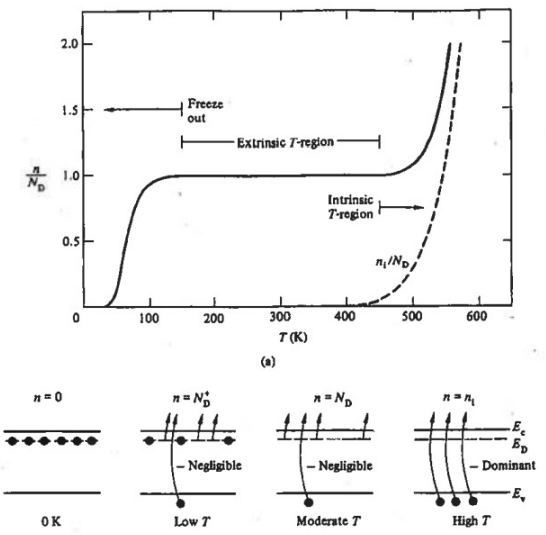

Fig. 2. Carrier concentration in n-type doped semiconductors as a function of temperature, from [5], p. 66

states and the material is an insulator. Increasing the temperature and e^- are supplied to the conduction band by the shallow donor atoms at an essentially exponential rate:

$$n \cong \left(\frac{N_D N_C}{2}\right)^{1/2} exp\left(-\frac{E_D^b}{2k_B T}\right) \tag{16}$$

The Fermi level is then approximately

$$E_F \cong E_C - \frac{E_D^b}{2} + \frac{k_B T}{2} \ln\left(\frac{N_D}{\hat{g}_D N_C}\right). \tag{17}$$

- *Extrinsic region (moderate T):*
  Now that all the donors are ionized, the carrier concentration will be roughly constant, $n \approx N_D$.
- *Intrinsic region (high T):*
  For large Temperatures, n will asymptotically approach the intrinsic concentration, n_i, for the thermal energy is large enough to supply a large amount of electrons previously bound to the host atoms. Since the probability of their supplementation into the conduction band has an exponential dependence on the Temperature, this insertion process is becoming more and more dominant over the donator atom insertion, $n = n_i$.

To estimate the donator state energy level E_D, the linear region in the plot $n/T^{3/4}$ vs. $1/T$ needs to be interpolated. Indeed, in the freeze out region, the ionization energy E_D^b can be found using:

$$ln\left(\frac{n}{T^{3/4}}\right) = A + \frac{B}{T} \tag{18}$$

where A and B are constants. We are specifically interested in B, since $E_D^b = -2k_B B$. The physical significance of A is that it encodes the doping concentration N_D. Indeed, N_D can be obtained using $N_D = \left(\frac{2\pi\hbar^2}{m_e k_B}\right)^{3/2} \exp(2A)$.

From the temperature dependence of the mobility several kinds of scattering mechanisms can be identified. The origins of different scattering rates of the charge carriers as a function of temperature are summarized in Table I, obtained from [9].

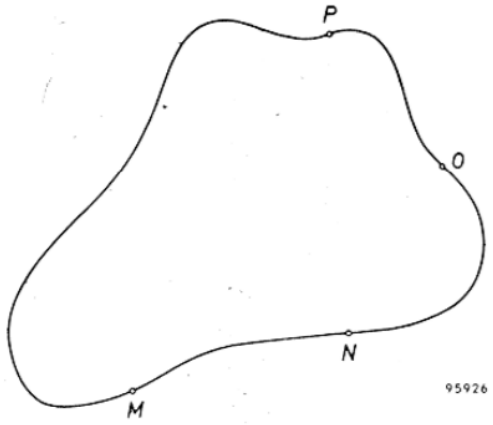

Fig. 3. two-dimensional lamella, from [4]

3) Van der Pauw - Geometry: Van der Pauw first described the Hall effect measurement for samples of (almost) arbitrary shape in 1958 in [3] and [4]. The results can be summarized as follows:

- The sample needs to have an approximately two-dimensional shape (meaning it's width needs to be much larger than it's height).
- The sample cannot contain any holes.
- The four electrodes need to be as close as possible to the perimeter of the sample. Furthermore, the contact areas should be at least one order in magnitude smaller than the sample area.
- The sample should have a uniform thickness d and must be homogeneous and isotropic.
- It is preferred that the sample has a line of symmetry.

Two of the four contacts are then used to measure a voltage drop between them, while the other two allow a current to flow. In his publication, van der Pauw used a sample with the shape shown in Fig. (3).

He showed that, defining the following "resistances"

$$R_{MN,OP} = \frac{V_P - V_O}{I_{MN}} \tag{19}$$

$$R_{NO,PM} = \frac{V_M - V_P}{I_{NO}} \tag{20}$$

the (average) resistivity can be calculated by

$$\rho = \frac{\pi d}{\ln 2} \frac{R_{MN,OP} + R_{NO,PM}}{2} f. \tag{21}$$

f is a slowly varying function, dependant on the ratio of the two resistances (19), (20). For our purposes, the correction function can be taken to be 1.

Furthermore, Van der Pauw showed that the Hall coefficient can be measured in this setup. Firstly, the value of $R_{MN,OP}$ needs to be noted, after which a uniform magnetic induction B was turned on, at right angles to the surface. This changes the resistance by an amount ΔR which then serves to write down the Hall coefficient as:

TABLE I

Scattering mechanisms for mobility and temperature dependence		
Scattering Mechanism	**Functional Dependence**	**Validity**
Ionized Impurity Scattering	$\mu \propto T^{3/2}$	Most prevalent in covalent semiconductors like Si or Ge at low temperatures.
Deformation Potential Scattering	$\mu \propto T^{-3/2}$	Most prevalent in covalent semiconductors at high temperatures.
Piezoelectric Potential Scattering	$\mu \propto T^{-1/2}$	Most prevalent in piezoelectric and strongly ionic crystals, like the $II-IV$ semiconductors like ZnO or $ZnSe$. Scattering can be stronger then the deformation potential scattering.
Polar Optical Scattering	$\mu \propto \exp\left(\frac{\Theta_D}{T}\right)$	For $T \ll \Theta_D$, where Θ_D is the Debye temperature. Most prevalent in bulk polar semiconductors like ZnO or $GaAs$ at room temperature.
Dislocation Scattering	$\mu \propto \frac{\sqrt{n}}{N_{disl}} T$	Irregularities from the perfectly periodic crystal potential, like dislocations, can contain charge centres and can act as scattering centres. It is a very common scattering mechanism in samples that have deformed.
Grain Boundary Scattering	$\mu \propto T^{-1/2} \exp\left(-\frac{\Delta E_b}{k_B T}\right)$	Where ΔE_b is the electronic barrier. Important effect in polycrystalline materials and thin films. Dependant on the doping concentration.

$$R_H = \frac{d}{B}\Delta R. \tag{22}$$

B. Experimental Setup and Data Analysis

The measurements were mostly run automatically. The software initializes the measurement devices and determines the maximal current for which the heating of the electrodes (Ohmic heating) and the Peltier effect had negligible effects on the measured quantities. The maximal current thus determined I_{max} and another, one to two orders of magnitude smaller current, were utilized to obtain the Van der Pauw resistances, eqns. (19) (20).

The program averages 400 single measurements for each of the 16 voltage measurement setups. The recordings are then saved for later analysis, together with readily available standard deviations.

Plotting and fitting the results was mostly done using Python Scripts. All obtained values are then given with the computed standard deviations from the fits.

C. Material Information

For the Hall measurement, we obtained data for three different samples:

1) ZnO $(E927)$
2) CuI $(C440-2)$
3) ZTO $(E3266)$

The temperature dependant measurements were given for a PLD ZnO thin film and a ZnO bulk sample. Both probes were grown on an Al_2O_3 substrate and had thicknesses of $500\mu m$ (bulk) and $10\mu m$ (thin film). Hall Corners were then sputtered onto the samples for the Hall measurements.

III. Results and Discussion

A. Hall effect

Our results are shown in Table II. The majority charge carrier type is given by the sign of the Hall coefficient. Hence, ZnO and CuI are both n-type semiconductors, while ZTO is a p-type semiconductor. The CuI sample shows quite high standard deviations, suggesting an inhomogeneous sample. The measurements for the other samples yield values that are independent of the currents and within reasonable, to be expected, orders of magnitude.

B. Temperature dependent measurement

From Fig. 4, the slope of the linear model was $-203.01K$. Hence the thermal activation energy E_1 is calculated to be $E_1 = 35.0 \pm 0.5meV$. The impurities are rather shallow, typically thermal activation energies lie between 35 and 120 meV [10]. From the intercept, the donor concentration was calculated to be $N_D = (1.17 \pm 0.05) \times 10^{17} cm^{-3}$.

The mobility and it's most important scattering mechanisms are shown in Fig. 5. Hence, for low temperatures, *ionized impurity scattering* dominates the behaviour of μ, while for intermediate temperatures, the *piezoelectric* and for high temperatures, the *deformation potential* constrain the mobility. This agrees with the experimental data in [10] which predicts that for even larger temperatures, the mobility is further constrained by polar optical scattering processes due to optical phonons. This deviation is also seen in Fig. 6, which is an enhanced view of Fig. 5.

C. Correction for thin film probes

To avoid lattice mismatch between substrate and bulk sample, a thin inter-facial region is often sputtered or grown onto the substrate. However, as [11] suggests this will non-linearly affect the conductivity and hence the obtained donor

TABLE II

Hall coefficients and resistivities for different samples				
Compound $(I(A))$	$R_H(m^3/As)$	$\rho(\Omega m)$	n or $p(cm^{-3})$	$\mu\ (cm^2/Vs)$
ZnO (2.0×10^{-4})	9.280×10^{-6}	3.05×10^{-3}	6.73×10^{17}	30.42
ZnO (7.0×10^{-4})	9.276×10^{-6}	3.05×10^{-3}	6.73×10^{17}	30.41
CuI (1.5×10^{-6})	1.209×10^{-5}	3.18×10^{-4}	5.16×10^{17}	380.19
CuI (6.9×10^{-6})	1.135×10^{-5}	3.89×10^{-4}	5.50×10^{17}	291.8
ZTO (2.0×10^{-3})	-2.378×10^{-7}	1.91×10^{-4}	2.62×10^{19}	-12.45
ZTO (1.0×10^{-4})	-2.371×10^{-7}	1.91×10^{-4}	2.63×10^{19}	-12.41

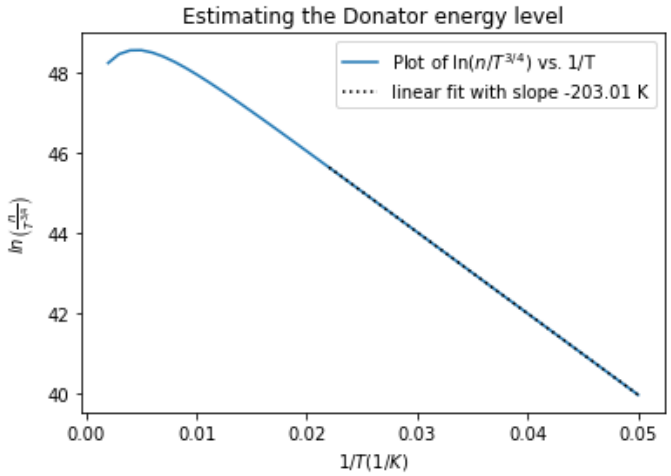

Fig. 4. For sufficiently low Temperatures, the plot of $\ln\left(\frac{n}{T^{3/4}}\right)$ appears linear.

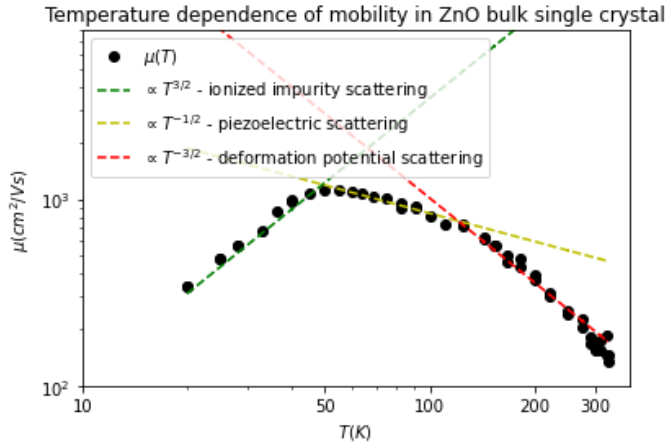

Fig. 5. mobility μ vs T. The scattering mechanisms are shown as dashed lines.

concentration and thermal activation energies. A two-layer analysis for the Hall effect is presented and the authors conclude the following corrections: At very low temperatures $(T < 40K)$ the degenerate interface layer is solely responsible for carrier flow with a conduction that is very *metal-like*. It follows that n_2 and μ_2 can be easily read off from the low temperature Hall data and can be used to calculate the electron

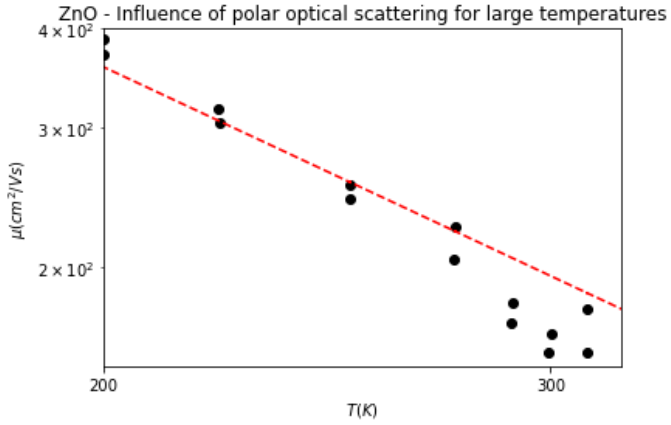

Fig. 6. mobility μ vs T for large temperatures. Close to room temperature, μ is further decreased by the polar optical scattering mechanism.

concentration n_1 and the mobility μ_1 of layer 1:

$$n_1(T) = \frac{(\mu_H^2 n_H - \mu_2^2 n_{\square 2}/d)^2}{\mu_H^2 n_H - \mu_2^2 n_{\square 2}/d} \tag{23}$$

$$\mu_1(T) = \frac{\mu_H^2 n_H - \mu_2^2 n_{\square 2}/d}{\mu_H n_H - \mu_2 n_{\square 2}/d} \tag{24}$$

The results are shown in Fig. 10 and 11. Exponential fits of the form AT^B were performed in two separate temperature domains. Fig. 7 shows the behaviour of the mobility at low and at high temperatures.

For the high temperature regime, the fit with exponent $B = -1.30 \pm 0.03$ is reasonably close to $-3/2$ and hence the deformation potential is again inhibiting the mobility the most for high temperatures. For low temperatures however, the power law with exponent $B = 2.5 \pm 0.1$ can be associated with dislocation scattering for temperatures between $\approx 60K$ and $\approx 100K$, since the temperature dependence of the carrier concentration follows a roughly cubic *empirical* dependence (see Fig. 8) for this region. Grain boundary scattering can also be fitted to the temperature range in question (see Fig. 9), where we determined the electronic barrier has a typical value [12] of $\Delta E_b = (12.4 \pm 0.5) meV$.

In ZnO thin films, the mobility has previously been shown to be

Similarly to above, the slope of $\ln\left(\frac{n}{T^{3/4}}\right)$ vs. $1/T$ (see Fig. 12) contained information for the donor atom binding energy: $E_1 = 37 \pm 1 meV$, while the intercept led to an estimation for the donor concentration of $N_D = (1.70 \pm 0.05) \times 10^{18} cm^{-3}$. The result is in relative proximity to the previously determined binding energy and leads to the conclusion that the

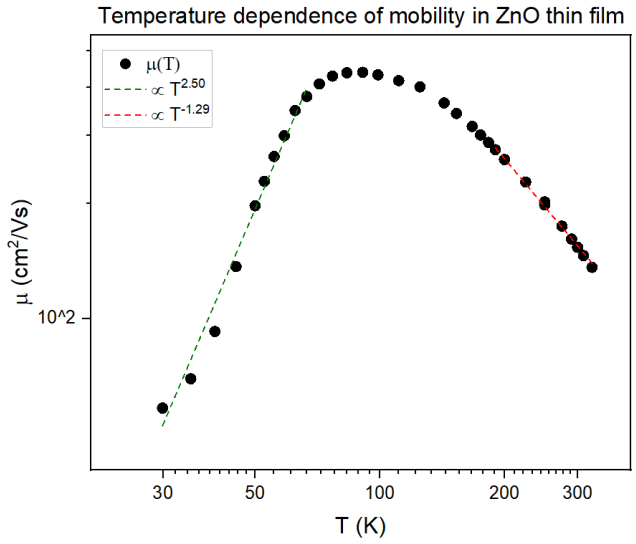

Fig. 7. The corrected carrier mobility and corresponding scattering dependencies as dashed lines.

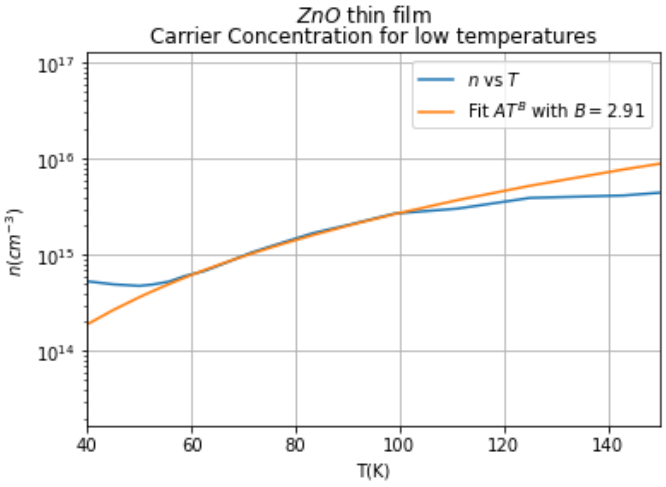

Fig. 8. Carrier Concentration for low temperatures, in regime of dislocation scattering, i.e. between $\approx 60K$ and $\approx 100K$, the carrier concentration is roughly cubically dependent on the temperature.

probes contain the same donor atoms. A paper from 2002 by Hofmann et. al. [13] suggests that the corresponding donor could be Hydrogen. In their paper, they found an ionization energy of $E_D^b = 35meV$. [10] also reported an ionization energy of $E_D^b = 37 \pm 2meV$ for H_i. Hydrogen is a very common (unintentional) donor in ZnO, making it an n-type semiconductor [14]. Indeed, efforts are being made to obtain p-type ZnO, which proved to be quite difficult in the past.

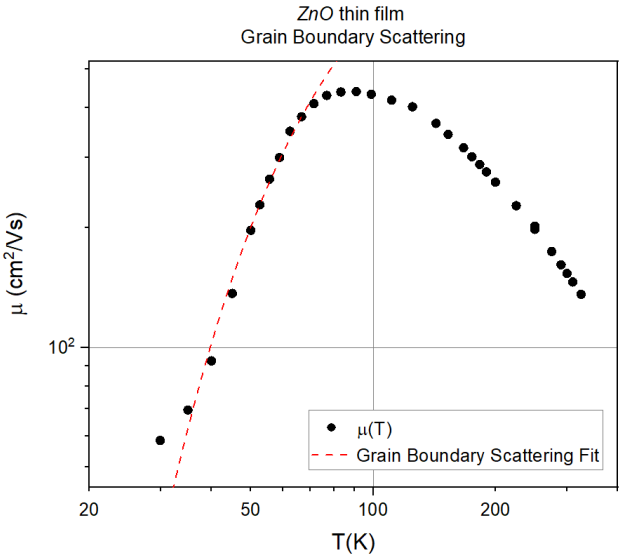

Fig. 9. For low temperatures, the mobility is limited by grain boundary scattering.

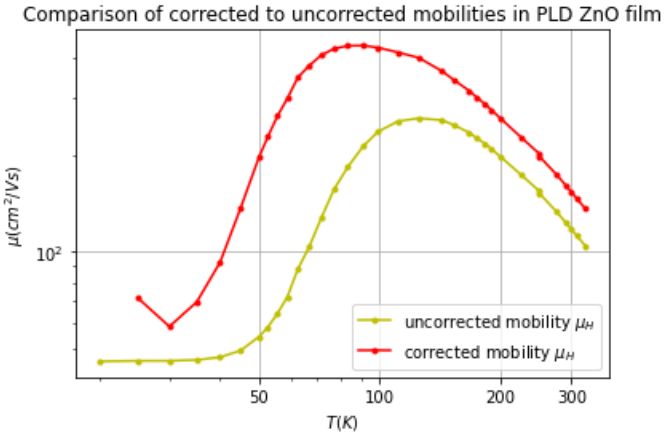

Fig. 10. The effect of the two-layer analysis on the mobility μ_H. The measured mobility systemically underestimates the actual mobility.

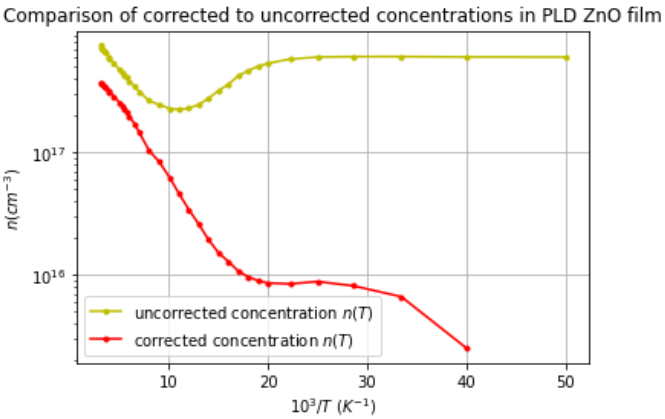

Fig. 11. The uncorrected carrier concentration can be seen to saturate at a constant level of $n \approx 5 \times 10^1 7cm^{-3}$ for low temperatures. Without the two-layer analysis, this would falsely imply that there is a second deeper lying donor level in the sample.

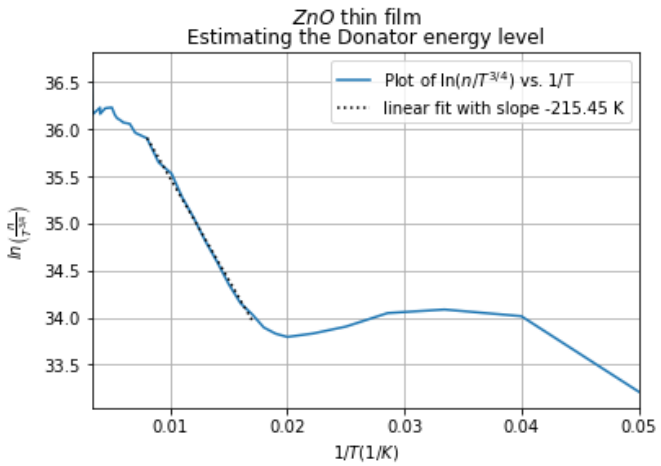

Fig. 12. As performed for the bulk sample, the linear fit can be used to obtain values for the donor concentration N_D and the ionization energy E_D^b.

REFERENCES

[1] K. Kopitzki, P. Herzog, 2017, *Einführung in die Festkörperphysik*, 7th edition, Heidelberg: Springer Spektrum.

[2] F. J. Morin, J. P. Maita: Phys. Rev. 96, 29 (1954)

[3] L.J. van der Pauw, 1958, *A method of measuring specific resistivity and Hall effect of discs of arbitrary shape*, Philips Research Reports. 13: 1–9.

[4] L.J. van der Pauw, 1958, *A method of measuring the resistivity and Hall coefficient on lamellae of arbitrary shape*, Philips Technical Review. 20: 220–224.

[5] R. Pierret, 1996, *Semiconductor Device Fundamentals*, 1st edition, Boston: Addison-Wesley Publishing Cempany, Inc

[6] D.P. Norton, Y.W. Heo, M.P. Ivill, K. Ip, S.J. Pearton, M.F. Chisholm, T. Steiner, *ZnO: growth, doping & processing*, Materials Today, Volume 7, Issue 6, 2004, Pages 34-40, *https://doi.org/10.1016/S1369-7021(04)00287-1*.

[7] Oshikiri, M. and Imanaka, Y. and Aryasetiawan, F. and Kido, Giyuu, *Comparison of the electron effective mass of the n-type ZnO in the wurtzite structure measured by cyclotron resonance and calculated from first principle theory*, Physica B-condensed Matter, April, 2001, Pages 472-476, *https://doi.org/10.1016/S0921-4526(01)00365-9*

[8] Fan, Z.; Lu, J. G. J. Nanosci. Nanotechnol. 2005, 5, 1561.

[9] Marius Grundmann. *The Physics of Semiconductors: An Introduction Including Nanophysics and Applications*, Springer, Heidelberg, third edition, 2016.

[10] von Wenckstern H. et al. *Donor Levels in ZnO*. In: Kramer B. (eds) Advances in Solid State Physics. Advances in Solid State Physics, vol 45. Springer, Berlin, Heidelberg, *https://doi.org/10.1007/11423256_21*.

[11] D. C. Look, R. J. Molnar, *Degenerate layer at GaN/sapphire interface: Influence on Hall-effect measurements*, Appl. Phys. Lett. 70, 3377-3379 (1997) *https://doi.org/10.1063/1.119176*

[12] J.W. Orton, M.J. Powell, *The Hall effect in polycrystalline and powdered semiconductors*. Rep. Prog. Phys. 43, 1263–1307 (1980)

[13] Detlev M. Hofmann et. al, *Hydrogen: A Relevant Shallow Donor in Zinc Oxide*, Phys. Rev. Lett. 88, 045504 (2002) *https://doi.org/10.1103/PhysRevLett.88.045504*

[14] Titao Li, Mengye Wang, Xiaolong Liu, Mingge Jin, and Feng Huang, *Hydrogen Impurities in ZnO: Shallow Donors in ZnO Semiconductors and Active Sites for Hydrogenation of Carbon Species* The Journal of Physical Chemistry Letters 2020 11 (7), 2402-2407 DOI: 10.1021/acs.jpclett.0c00509